AUSTRALIAN JOURNAL OF BASIC AND APPLIED SCIENCES

ISSN:1991-8178 EISSN: 2309-8414
Journal home page: www.ajbasweb.com

Vibration Analysis Of Cnt Composites For Aerospace Applications

[1]G. Yellam Raju, [2]G. Amarnath, [3]Dr. N. Venkatachalapathi

[1]*Student, Mechanical Engineering, AITS, Rajampet, AP*
[2]*Assistant Professor, Mechanical Engineering, AITS, Rajampet, AP*
[3]*HOD, Mechanical Engineering, AITS, Rajampet, AP*

Address For Correspondence:
G.Yellam Raju, Student, Mechanical Engineering, AITS, Rajampet, AP,
E-mail: yellamraju1827@gmail.com

ARTICLE INFO

Article history:
Received 18 June 2017
Accepted 28 July 2017
Available online 20 August 2017

Keywords:
CNT/C composites, curved fibber, vibration analysis, ansys.

ABSTRACT

Now A Days Composites Are Playing Major Role ,Aerospace Application .Generally We Have Carbon Fibber Carbon Composites. In This Work We Introduce CNT Fibber, Carbon Matrix Composites. Present Smart Material Trend Is Going On, Carbon Nanotube Having High Thermal Resistance, High Strength Low Density And Extremely Low Coefficient Of Thermal Expansion With Compare To The Carbon Fibber. Make Carbon Nanotubes A Promising Substitute For Carbon Fibres To Meet The Challenges Of The Next Generation Aerospace Technologies. In This Work We Using Curved Fibber Why Because We Get High Surface Finishing .This Materials Very Use Full For Aerospace Applications. The Assumption Of Von Karman's Nonlinear Thin Plate Theory Made. And Also Considered 8 Ply Laminated Composite. Find The Analytical Nonlinear Frequency With Compare To The Numerical Solution.

INTRODUCTION

Carbon fibre reinforced carbon matrix (C/C) composites have attracted tremendous attention from aerospace industries due to their high temperature resistance, high strength, low density, and extremely low coefficient of thermal expansion. Compared with carbon fibers, carbon nanotubes (CNTs)possess theoretical strengths that are up to an order of magnitude ehigher, as well as much higher electrical and thermal conductivities. These excellent properties, combined with the high specific surface area, make carbon nanotubes a promising substitute for carbon fibres to meet the challenges of the next generation aerospace technologies .Inspired by the processing methods of C/C composites, chemical vapor infiltration (CVI) and polymer infiltration phyrolysis (PIP) methods have been explored to synthesize CNT/C composites. Existence of CNTs was found to induce graphitization in the matrix under high temperatures. Increase in CNT content and degree of alignment were also found to assist the formation of graphite regions . However, the tensile strength and Young's modulus of previously reported CNT/C composites are far lower than those of their C/C counterparts. In addition, the electrical properties were not investigated in detail. Challenges in preparing CNT/C composites with desirable properties include achieving CNT alignment in the structure and homogeneous CNT dispersion in the carbon matrix. In our previous work, we developed a one-step winding infiltration method to utilize long and aligned CNT sheets and produced high strength CNT/polymer composites .This method has a unique advantage in producing aligned CNT composite structures, in which nanotubes are uniformly distributed in the matrix. In this current work, we applied this method to fabricate CNT/polyacrylonitrile (PAN) precursor composites and then pyrolyzed the PAN matrix to make aligned-structured CNT/C composites. PAN is a commercially important polymer, which is used as the predominant precursor for carbon fibers. PAN has the advantages of high carbon yield, simple carbonization process and the ability for surface functionalization. CNTs have been added to PAN fibres in small quantities to improve their properties .Other works have studied the stabilization and carbonization of similar materials, which has been proposed as the next generation carbon fibre products.

To Cite This Article: G. Yellam Raju, G. Amarnath, Dr. N. Venkatachalapathi., Vibration Analysis Of Cnt Composites For Aerospace Applications. ***Aust. J. Basic & Appl. Sci.,*** *11(11): 48-59, 2017*

While that method is very promising for producing carbon fibers, there is a growing interest in making composites that contain no carbon fibres and only a high fibre volume fraction of CNTs as the reinforcing phase. However ,there are only limited studies on PAN/C composites films or CNT/C composites produced directly from CNT structures. Producing CNT/C composites by dispersing short CNTs with random orientation and entanglements into carbon precursors and then carbonizing it typically results invery brittle and weak composites .This work presents a new technique to produce CNT/C composites directly from aligned CNT sheets and PAN precursor ,which exhibit mechanical properties superior to other CNT/C composites that are not in a fibre form. The CNT/PAN precursor composite were stabilized, carbonized and further graphitized to produce CNT/C composites. The morphology and mechanical properties were investigated in both the precursor and carbonized states. Raman spectroscopy and electrical properties of the precursor, carbonized and graphitized composites were also analyzed.

Types of nanotubes:

Generally two types of nanotubes

- Single wall nanotubes
- multi wall nanotubes

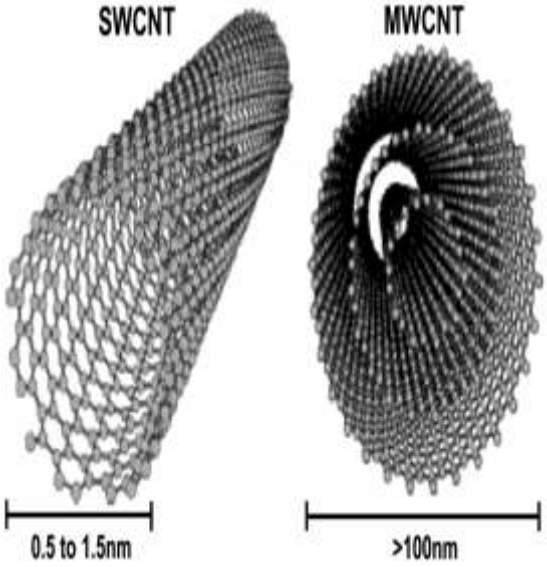

Construction of cnt:

Structurally, SWNTs can be compared to ‘‘rolled up’’ oneatom-thick sheets of graphite called grapheme. The way the graphene is wrapped along the honeycomb grapheme structure is given by chiral vector ~C which is a result of a pair(n,m) of integers that correspond to graphene vectors ~a1 and ~a2.The principle of SWNT construction from a graphene sheet along the chiral vector ~C is shown in Fig. 2. There are two standard types of SWNTs constructions from a single grapheme sheet according to integers (n,m) . The (n,0) structure is called ‘‘zigzag’’ and the structure where n ¼ m (n,n) is called ‘‘armchair’’. The third non-standard type of CNTs construction, which can be characterized by the equation where n > m > 0, is called ‘‘chiral’’ .The chirality predestinates the electrical, mechanical, optical andother properties of CNTs. For example Dresselhaus et al.reported how the chiral vector and the corresponding pairs of integers influence the electrical properties of CNTs.6CNTs can be constructed in two basic forms, SWNTs and MWNTs. SWNTs consist of a single tube of grapheme, whereas MWNTs are composed of several concentric tubes of graphene fitted one inside the other. The diameter of CNT svaries from a few nanometres in the case of SWNTs to several tens of nanometres in the case of MWNTs. The lengths of the CNTs are usually in the micrometre range.7 The simplest example of MWNTs is double walled carbon nanotubes

Types of Composites:

Generally we have 4 types of composites

1. PMC’S
2. CMC’S
3. C-C composites
4. MMC’S

Graphene:

In simple terms, graphIne is a thin layer of pure carbon; it is a single, tightly packed layer of carbon atoms that are bonded together in a hexagonal honeycomb lattice

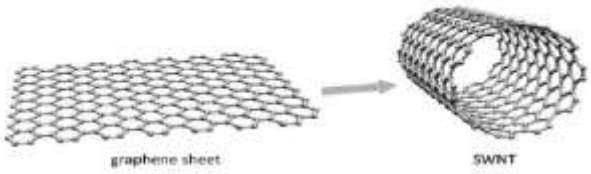

2.Objectives:

Mechanical properties for materials typically used for lightweight aerospace structures shown. Data points for IM7 and M46J are representative of carbon fibre tensile properties. While these fibres exhibit excellent tensile properties, the carbon fibre reinforced polymer (CFRP) composites produced from them have much lower mechanical properties. This knockdown in properties prevents the full realization of carbon fibre's potential to enable structural weight savings. Plotted on the same graph, the nano scale tensile properties of individual CNTs are so much higher than those of carbon fibres' that despite anticipated knockdowns in mechanical performance of the structural composites produced from them, significant mass reductions of structural components constructed from these composites were deemed to be a promising goal. If realized, these weight savings can enable more affordable space exploration. Exploiting carbon fibre strength in composites has been an area of interest for several decades, especially in aerospace applications where lightweight structures are paramount . With the advent of CNTs, this need for mass efficiency drove some of the extraordinary attention paid to the potential for these nano fillers to yield composites with mechanical properties that are competitive with those of CFRPs. Until recently, much of the work reported in the literature have been devoted to property enhancements possible with low loadings of CNTs in engineering polymer matrices such as epoxies and polyamides. Dispersing more than a few percent of CNTs in polymer matrices is challenging due to increased viscosities that result from adding these high surface area nano fillers to the polymer matrix. Several approaches to overcome this processing difficulty have been documented. Although investigations of lightly doped polymer matrices have yielded some understanding of processing approaches that can improve the nanotube /matrix interface to enhance load transfer.

Generally in aeroplane large number of vibration are produced, due to this effect cracks are formed near to glass frames and propeller casing. To avoid those problems by using CNT/C composites.

Table 1:

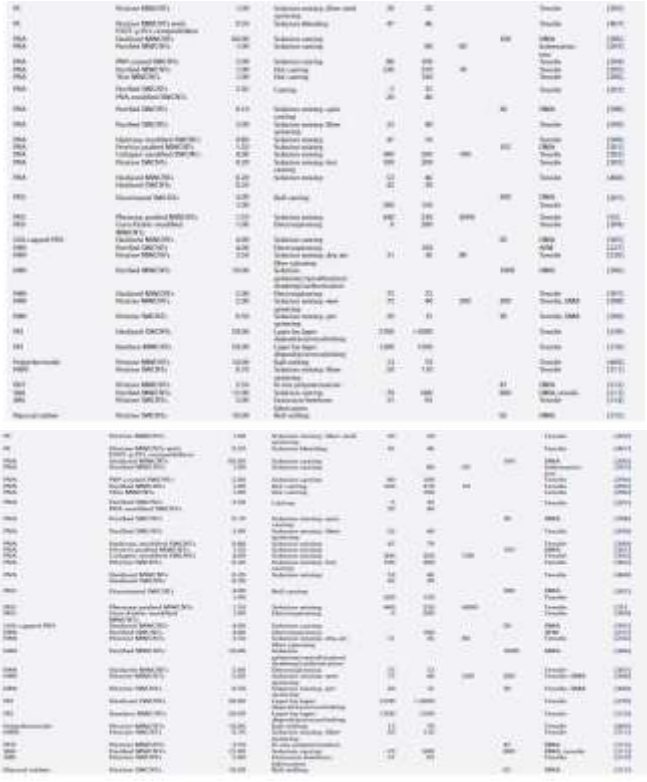

3.Literature Data:

Table 1 represents a comprehensive collection of published data in this field. The table is organized as follows the polymer matrices in column 1 are arranged by type .In column 2, CNT species (single/double/multi-walled) and state (pristine/oxidized/chemically modified) are given .Finally, in columns 3 and 4 the weight fraction of CNTs and the processing method are specified, respectively .Mechanical characteristics like tensile strength at break, elastic modulus and toughness of the composite materials are listed in columns 5–7, respectively (% change compared to the neat matrix). In addition, the % change of storage modulus of composites is given in column 8 (in cases where DMA technique was used). Finally, the type of mechanical testing (tensile, DMA, etc.) and the reference number are listed in columns 9 and 10, respectively. Inspection of Table 1 clearly shows a large spread in the number of investigations for different polymer matrices.

4.Methodology:

1) Analytical solution
2) Numerical analysis

Analytical Formulation:

Creation of laminates with curvilinear fibbers:

4.1. Description of the reference fibber path:

In contrast to conventional laminates with rectilinear fibbers, curvilinear fibber paths cannot be described by a single orientation angle. A wide range of freedom in describing the fiber path orientation is offered by adopting the convention in [15]. It is assumed that the reference fibber path orientation varies linearly with x from one value T0 at the centure to another value T1 at a distance a/2 from the origin, where a is the length of the rectangular laminate. The orientation of a single curvilinear fiber path is denoted by hT0/T1i. The reference fiber path and orientation are shown in Fig. 1. Since a ply is composed of fibre oriented similarly to the reference fiberpath, the description of the reference fibre path will serve to describe all fibers. A laminate composed of two adjacent plies with equal and opposite T0 and T1 is denoted by [_T0/T1] which means [+(T0/T1)-(T0/T1)]. The reference fiber path function y and orientation h can be expressed in terms of T0, T1, and x as

$$y=\begin{Bmatrix}\frac{a}{2(T_1-T_0)}\left\{-\ln[\cos(T_0)]+\ln\left[\cos\left(T_0-\frac{2(T_1-T_0)}{a}x\right)\right]\right\} for -a/2\le x\le 0\\ \frac{a}{2(T_1-T_0)}\left\{\ln[\cos(T_0)]-\ln\left[\cos\left(T_0+\frac{2(T_1-T_0)}{a}x\right)\right]\right\} for 0\le x-a/2\end{Bmatrix}$$

$$\theta=\arctan(y')=\begin{Bmatrix}-\frac{1}{a}(T_1-T_0)x+T_0\, for -a/2\le x\le 0\\ \frac{1}{a}(T_1-T_0)x+T_0\, for 0\le x\le a/2\end{Bmatrix}----------2$$

where y0 denotes the first derivative of y with respect to x.

4.2. Shifted fibre paths:

To create the remaining fibre paths, the reference fibre path is shifted fixed distances along the y axis. This process is straight forward .In contrast to parallel fibres where fibre paths are generated through a numerical scheme, shifted fibre paths possess analytical expressions. A [_h30/60i] laminate composed of shifted fibres is shown in Fig. 2. 2.3. Fibre curvature constraint To create laminates with curvilinear fibres, it is necessary to curve the tow paths. If a tow is curved too much, then it is possible that a kink will develop in the fibre. To avoid kinking, the magnitude of the largest curvature for any ply must be less than a prescribed maximum value. The shifted fibre paths are similar to the reference fibre path. Therefore, the curvature constraint is applied only to the reference fibre path. Since the reference fibre path function y is anti symmetric, only the curvature of this path in the positive x portion needs to be found. The curvature j for a curvilinear fibre path is defined as

$$k=\frac{y''}{[1+(y')^2]^{3/2}}----------3$$

where y00 denotes the second derivative of y with respect to x. The curvature of the reference fibre path in the positive x portion can be found by inserting the first and second derivatives of the fibre path function y in Eq. (3) as

$$k=\frac{2}{a}(T_1-T_0)\cos[T_0+\frac{2}{a}(T_1-T_0)x]----------4$$

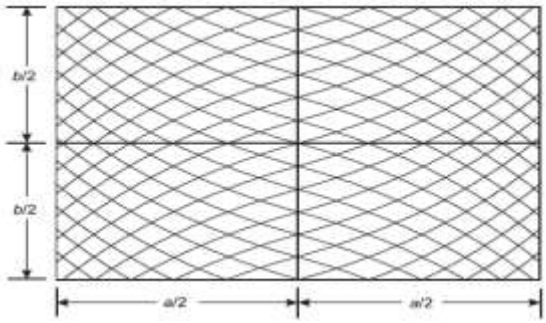

Fig. 2: [≠<30/60>] iaminate composed of shifted curvilinear fibers.

At each point along the fibre reference path, the magnitude of the curvature j must be less than the maximum prescribed value of 3.28 1/m (in [16], this value is given as 1/12 1/in). If the fibre curvature constraint is not satisfied, the ply cannot be manufactured .The design space for a shiftedfiber ply (a = 0.5 m) is shown in Fig. 3. The gray region is where the shifted fiber format is a valid design since the fibre curvature constraint is satisfied everywhere in this region.

5. Formulation:

5.1. Elastic properties:

The stress–strain relations for an orthotropic ply in the principal material directions under plane stress conditions are given by

$$\begin{Bmatrix}\sigma_{11}\\ \sigma_{22}\\ \tau_{12}\end{Bmatrix}=\begin{bmatrix}Q_{11} & Q_{12} & 0\\ Q_{12} & Q_{22} & 0\\ 0 & 0 & Q_{66}\end{bmatrix}\begin{Bmatrix}\varepsilon_{11}\\ \varepsilon_{22}\\ \gamma_{12}\end{Bmatrix}---------5$$

$$Q_{11}=\frac{E_1}{1-\nu_{12}\nu_{21}}---------6$$

$$Q_{22}=\frac{E_2}{1-\nu_{12}\nu_{21}}---7$$

$$Q_{12}=\nu_{12}Q_{22}=\nu_{21}Q_{11}-----8$$

$$Q_{66}=G_{12}----------9$$

In the above, the subscripts 1 and 2 refer to the fibre direction and the direction transverse to the fibre, respectively.

The stress–strain relations in the x and y directions are given by

$$\begin{Bmatrix}\sigma_{xx}\\ \sigma_{yy}\\ \tau_{xy}\end{Bmatrix}=\begin{bmatrix}\bar{Q}_{11} & \bar{Q}_{12} & \bar{Q}_{16}\\ \bar{Q}_{12} & \bar{Q}_{22} & \bar{Q}_{26}\\ \bar{Q}_{16} & \bar{Q}_{26} & \bar{Q}_{66}\end{bmatrix}\begin{Bmatrix}\varepsilon_{xx}\\ \varepsilon_{yy}\\ \gamma_{xy}\end{Bmatrix}---------10$$

Where

$$\bar{Q}_{11}=Q_{11}\cos^4(\theta)+2(Q_{12}+2Q_{66})\sin^2(\theta)\cos^2(\theta)+Q_{22}\sin^4(\theta)---11$$

$$\bar{Q}_{12}=(Q_{11}+Q_{22}-4Q_{66})\sin^2(\theta)\cos^2(\theta)+Q_{12}(\sin^4(\theta)+\cos^4(\theta))---12$$

$$\bar{Q}_{22}=Q_{11}\sin^4(\theta)+2(Q_{12}+2Q_{66})\sin^2(\theta)\cos^2(\theta)+Q_{22}\cos^4(\theta)-----13$$

$$\bar{Q}_{16}=(Q_{11}-Q_{12}-2Q_{66})\sin(\theta)\cos^3(\theta)-(Q_{22}-Q_{12}-2Q_{66})\sin^3(\theta)\cos(\theta)--14$$

$$\bar{Q}_{66}=|(Q_{11}+Q_{22}-2Q_{12}-+2Q_{66})\sin^2(\theta)\cos^2(\theta)+Q_{66}(\sin^4(\theta)+\cos^4(\theta))---16$$

$$\bar{Q}_{26}=(Q_{11}-Q_{12}-2Q_{66})\sin^3(\theta)\cos(\theta)-(Q_{22}-Q_{12}-2Q_{66})\sin(\theta)\cos^3(\theta)--15$$

5.2. Hierarchical finite element matrices:

The laminate is idealized as one rectangular hierarchical finite element. The non-dimensional local coordinates n and g are expressed in terms of the global coordinates x and y as

$$\xi = \frac{2X}{a} \text{--------17}$$

$$\eta = \frac{2y}{b} \text{----------18}$$

The in-plane displacements u and v and the out-of-plane displacement w are expressed as

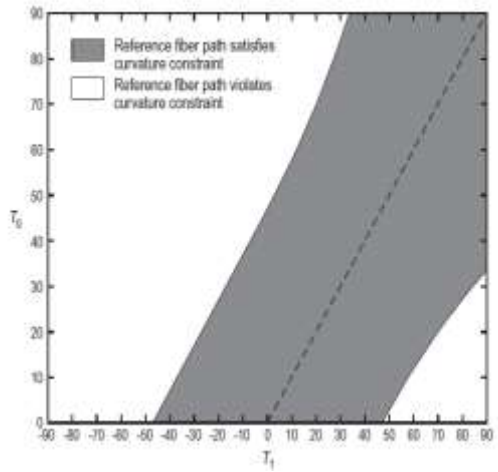

Fig. 3: Design space for ply composed of shifted curvilinear fibers (α=0.5m).

$$u = \sum_{k=1}^{p+1}\sum_{l=1}^{p+1} q_{2j-1}(t) g_k(\xi) g_1(\eta) \text{----19}$$

$$v = \sum_{k=1}^{p+1}\sum_{l=1}^{p+1} q_{2j}(t) g_k(\xi) g_1(\eta) \text{-----20}$$

$$w = \sum_{k=1}^{p+1}\sum_{l=1}^{p+1} q_j(t) f_k(\xi) f_1(\eta) \text{------21}$$

Where time and

J=l+(k-1)(p+1)----------22

The shape functions gi (i = 1,2,. . . ,p + 1) are given by

$$g_1(\xi) = \frac{1}{2}(1-\xi) \text{------23}$$

$$g_2(\xi) = \frac{1}{2}(1+\xi) \text{------24}$$

$$g_{j+1}(\xi) = \sqrt{\frac{2j-1}{2}} \int_{-1}^{\xi} p_{j-1}(\zeta) d\zeta \, (j = 2,3....., p) \text{-----25}$$

where Pj_1 is the Legendre orthogonal polynomial of order

j _ 1.

The internal shape functions gj+1 have the following two important properties:

$$g_{j+1}(-1) = g_{j+1}(1) = 0 \text{---26}$$

$$\int_{-1}^{1} \frac{dg_{i+1}(\xi)}{d\xi} \frac{dg_{j+1}(\xi)}{d\xi} d\xi = \begin{cases} 1 if i = j \\ 0 if i \neq j \end{cases} \text{------27}$$

The shape functions fi (i = 1,2,. . . ,p + 1) are given by

$$f_1(\xi)=\frac{1}{4}(2-3\xi+\xi^3)-----28$$

$$f_2(\xi)=\frac{1}{4}(1-\xi-\xi^2+\xi^3)----29$$

$$f_3(\xi)=\frac{1}{4}(2+3\xi-\xi^3)-------30$$

$$f_4(\xi)=\frac{1}{4}(-1-\xi+\xi^2+\xi^3)-----31$$

$$f_{j+1}(\xi)=\int_{-1}^{\xi} g_j(\zeta)d\zeta(j=4,5.....,p)----32$$

The internal shape functions fj+1 have the following two important properties:

$$f_{j+1}(-1)=f_{j+1}(1)=\frac{df_{j+1}(-1)}{d\xi}=\frac{dg_{j+1}(1)}{d\xi}----33$$

$$\int_{-1}^{1}\frac{d^2f_{i+1}(\xi)}{d\xi^2}\frac{d^2f_{j+1}(\xi)}{d\xi^2}d\xi=\begin{cases}1 if i=j\\0 if i\neq j\end{cases}------34$$

Explicit expressions for the functions gj+1 (j = 2,3,. . . ,10) and fj+1 (j = 4,5,. . . ,10) are available in [3].

The strain energy U of the hierarchical finite element is given by

$$\begin{aligned}U=\frac{1}{2}\int_{-1}^{1}\int_{-1}^{1}[&A_{11}\frac{b}{a}\left(\frac{\partial u}{\partial\xi}\right)^2+A_{22}\frac{a}{b}\left(\frac{\partial v}{\partial\eta}\right)^2+2A_{12}\frac{\partial u}{\partial\xi}\frac{\partial v}{\partial\eta}+A_{66}\frac{a}{b}\left(\frac{\partial u}{\partial\eta}\right)^2+A_{66}\frac{b}{a}\left(\frac{\partial v}{\partial\xi}\right)^2+2A_{66}\frac{\partial u}{\partial\eta}\frac{\partial v}{\partial\xi}\\&+2A_{16}\frac{\partial u}{\partial\xi}\frac{\partial v}{\partial\eta}+2A_{16}\frac{b}{a}\frac{\partial u}{\partial\xi}\frac{\partial v}{\partial\xi}+2A_{26}\frac{a}{b}\frac{\partial u}{\partial\eta}\frac{\partial v}{\partial\eta}+2A_{26}\frac{\partial v}{\partial\xi}\frac{\partial v}{\partial\eta}+2A_{66}\frac{\partial u}{\partial\eta}\frac{\partial v}{\partial\xi}-2B_{11}\frac{b}{a^2}\frac{\partial u}{\partial\xi}\frac{\partial^2 w}{\partial\xi^2}\\&-2B_{12}\frac{1}{b}\frac{\partial u}{\partial\xi}\frac{\partial^2 w}{\partial\eta^2}-4B_{16}\frac{1}{a}\frac{\partial u}{\partial\xi}\frac{\partial^2 w}{\partial\xi\partial\eta}-2B_{12}\frac{1}{a}\frac{\partial v}{\partial\eta}\frac{\partial^2 w}{\partial\xi^2}-2B_{22}\frac{a}{b^2}\frac{\partial v}{\partial\eta}\frac{\partial^2 w}{\partial\eta^2}-4B_{26}\frac{1}{b}\frac{\partial v}{\partial\eta}\frac{\partial^2 w}{\partial\xi\partial\eta}\\&-2B_{16}\frac{1}{a}\frac{\partial u}{\partial\eta}\frac{\partial^2 w}{\partial\xi^2}-2B_{16}\frac{b}{a^2}\frac{\partial v}{\partial\xi}\frac{\partial^2 w}{\partial\xi^2}-2B_{26}\frac{a}{b^2}\frac{\partial u}{\partial\eta}\frac{\partial^2 w}{\partial\eta^2}-2B_{26}\frac{1}{b}\frac{\partial v}{\partial\xi}\frac{\partial^2 w}{\partial\eta^2}-4B_{66}\frac{1}{b}\frac{\partial u}{\partial\eta}\frac{\partial^2 w}{\partial\xi\partial\eta}\\&-4B_{66}\frac{1}{a}\frac{\partial v}{\partial\xi}\frac{\partial^2 w}{\partial\xi\partial\eta}+4D_{11}\frac{b}{a^3}\left(\frac{\partial^2 w}{\partial\xi^2}\right)^2+4D_{22}\frac{a}{b^3}\left(\frac{\partial^2 w}{\partial\eta^2}\right)^2+8D_{12}\frac{1}{ab}\frac{\partial^2 w}{\partial\xi^2}\frac{\partial^2 w}{\partial\eta^2}+16D_{66}\frac{1}{ab}\left(\frac{\partial^2 w}{\partial\xi\partial\eta}\right)^2\\&+16D_{16}\frac{1}{a^2}\frac{\partial^2 w}{\partial\xi^2}\frac{\partial^2 w}{\partial\xi\partial\eta}+16D_{26}\frac{1}{b^2}\frac{\partial^2 w}{\partial\eta^2}\frac{\partial^2 w}{\partial\xi\partial\eta}+2A_{11}\frac{b}{a^2}\frac{\partial u}{\partial\xi}\left(\frac{\partial w}{\partial\xi}\right)^2+2A_{22}\frac{a}{b^2}\frac{\partial v}{\partial\eta}\left(\frac{\partial w}{\partial\eta}\right)^2\\&+2A_{12}\frac{1}{b}\frac{\partial u}{\partial\xi}\left(\frac{\partial w}{\partial\eta}\right)^2+2A_{12}\frac{1}{a}\frac{\partial v}{\partial\eta}\left(\frac{\partial w}{\partial\xi}\right)^2+4A_{16}\frac{1}{a}\frac{\partial u}{\partial\xi}\frac{\partial w}{\partial\xi}\frac{\partial w}{\partial\eta}+2A_{16}\frac{1}{a}\frac{\partial u}{\partial\eta}\left(\frac{\partial w}{\partial\xi}\right)^2+4A_{66}\frac{1}{b}\frac{\partial u}{\partial\eta}\frac{\partial w}{\partial\xi}\frac{\partial w}{\partial\eta}\\&+4A_{66}\frac{1}{a}\frac{\partial v}{\partial\xi}\frac{\partial w}{\partial\xi}\frac{\partial w}{\partial\eta}+4A_{26}\frac{1}{b}\frac{\partial v}{\partial\eta}\frac{\partial w}{\partial\xi}\frac{\partial w}{\partial\eta}+2A_{26}\frac{1}{b}\frac{\partial v}{\partial\xi}\left(\frac{\partial w}{\partial\eta}\right)^2+2A_{26}\frac{a}{b^2}\frac{\partial u}{\partial\eta}\left(\frac{\partial w}{\partial\eta}\right)^2+2A_{16}\frac{b}{a^2}\frac{\partial v}{\partial\xi}\left(\frac{\partial w}{\partial\xi}\right)^2\\&+A_{11}\frac{b}{a^3}\left(\frac{\partial w}{\partial\xi}\right)^4+A_{22}\frac{a}{b^3}\left(\frac{\partial w}{\partial\xi}\right)^4+2(A_{12}+2A_{66})\frac{1}{ab}\left(\frac{\partial w}{\partial\xi}\right)^2\left(\frac{\partial w}{\partial\eta}\right)^2+4A_{16}\frac{1}{a^2}\left(\frac{\partial w}{\partial\xi}\right)^3\frac{\partial w}{\partial\eta}\\&+4A_{26}\frac{1}{b^2}\frac{\partial w}{\partial\xi}\left(\frac{\partial w}{\partial\eta}\right)^3]d\xi d\eta-----35\end{aligned}$$

where Aij, Bij, and Dij are the stretching, stretching-bending coupling, and bending stiffness coefficients, respectively. They are given by

$$A_{IJ}=\sum_{K=1}^{N}(Z_{k+1}-Z_k)\bar{Q}_{ij}^{(k)}-----36$$

$$B_{IJ}=\frac{1}{2}\sum_{K=1}^{N}(Z^2{}_{k+1}-Z^2{}_k)\bar{Q}_{ij}^{(k)}-----37$$

$$D_{IJ}=\frac{1}{3}\sum_{K=1}^{N}(Z^3{}_{k+1}-Z^3{}_k)\bar{Q}_{ij}^{(k)}------38$$

where N is the number of plies.

The kinetic energy T of the hierarchical finite element is given by

$$T=\frac{1}{8}\rho abh\int_{-1}^{1}\int_{-1}^{1}\left[\left(\frac{\partial u}{\partial t}\right)^2+\left(\frac{\partial v}{\partial t}\right)^2+\left(\frac{\partial w}{\partial t}\right)^2\right]d\xi d\eta---39$$

where q is the averaged mass density.

The stiffness coefficients Aij, Bij, and Dij are function of n for curvilinear fibbers.

Using Hamilton's principle, the equations of free motion are obtained as

$$\overline{M_{ij}}\frac{d^2\overline{q_j}}{dt^2}+\overline{K_{ij}}\overline{q_j}+\left[\overset{\cup}{K}_{ij}+\hat{K}_{ij}\right]q_j=0----40$$

$$M_{ij}\frac{d^2q_j}{dt^2}+[K_{IJ}+\overset{\approx}{K}]q_j+\left[\overset{\cup}{K^T}_{ij}+2\overset{\wedge}{K^T}_{ij}\right]\overline{q_j}=0----41$$

Where

$$\overline{K_{ij}}=\begin{bmatrix}\overline{K}_{2I-1,2J-1} & \overline{K}_{2I-1,2J}\\ \overline{K}_{2I,2J-1} & \overline{K}_{2I,2J}\end{bmatrix}-----42$$

$$\overset{\cup}{K}_{ij}=\begin{bmatrix}\overset{\cup}{K}_{2i-1j}\\ \overset{\cup}{K}_{2IJ}\end{bmatrix}-------43$$

$$\hat{K}_{ij}=\begin{bmatrix}\hat{K}_{2i-1j}\\ \hat{K}_{2IJ}\end{bmatrix}-----44$$

$$\overline{q_j}=\begin{Bmatrix}\overline{q}_{2J-1}\\ \overline{q}_{2J}\end{Bmatrix}------45$$

$$I=j+(i-1)(p+1)------46$$

(I,j=1,2,…….,p+1)

The entries of the element matrices KI;J ; KI;J ; MI;J ; KI;J ; bKI;J , and eKI;J are given in Appendix A.Applying boundary conditions by ignoring the lines and columns associated with restrained degrees of freedom, the equations of free motion will be written as

$$\overline{M}\frac{d^2\overline{q}}{dt^2}+\overline{K}\overline{q}+\left[\overset{\cup}{K}+\hat{K}\right]q=0------47$$

$$M\frac{d^2q}{dt^2}+[K+\overset{\approx}{K}]q+\left[\overset{\cup}{K^T}+2\overset{\wedge}{K^T}\right]\overline{q}=0----48$$

If the plate's edges are immovable in the plane, the in-plane displacements become negligible in comparison with the out-of-plane displacement. Thus, the in-plane inertia may be neglected and the equations of motion uncoupled.

Neglecting in-plane inertia, Eq. (47) yields

$$\overline{q}=-\overline{K}^{-1}\left[\overset{\cup}{K}+\hat{K}\right]q----49$$

Inserting Eq. (49) into Eq. (48) gives

$$M\frac{d^2q}{dt^2}+\left[K-\overset{\cup}{K}^T\overline{K}^{-1}\overset{\cup}{K}+\overset{\approx}{K}-2\hat{K}^T\overline{K}^{-1}\hat{K}-\overset{\cup}{K}^T\overline{K}^{-1}\hat{K}-2\hat{K}^T\overline{K}^{-1}\overset{\cup}{K}\right]q=0---50$$

The force vectors bKTK_1K ^ q and K ^ TK_1 bKqare quadratic functions of q, whereas the force vectors eKq and bKTK_1 bKq are cubic functions of q.

Assuming

$$q=Q\cos(\omega t)----51$$

where ω is the frequency, and inserting Eq. (51) into Eq. (50) yields a system of equations of the form

$$F(\omega,t)=0----52$$

Applying the harmonic balance method to Eq. (52) yields

$$\frac{\omega}{\pi}\int_0^{2\pi/\omega} F(\omega,t)\cos(\omega t)dt = \left[\omega^2 M + K - \overset{\cup}{K}^T \overline{K}^{-1} \overset{\cup}{K} + \frac{3}{4}\overset{\approx}{K} - \frac{3}{4}\overset{\Lambda}{K}^T \overline{K}^{-1} \overset{\Lambda}{K}\right] Q = 0 \quad -----53$$

The stiffness matrix eK arises from the nonlinear in-plane strains only. The stiffness matrix bK TK_1bK represents coupling between linear and nonlinear in-plane strains. The stiffness matrix K ^ TK_1K ^ represents coupling between linear in-plane strains and curvatures. Eq. (53) is solved iteratively using the linearized updated mode method. In the first iteration, Q0 = 0 is assumed. In the successive iterations, the nonlinear stiffness matrices bK and eK are evaluated from the eigenvectors which are scaled so that the maximum amplitude matches the one specified. The resultant sparse generalized eigenvalue problem can be solved efficiently using the preconditioned conjugate gradient method [17]. The iteration process is continued until a converged value for the nonlinear frequency within the prescribed accuracy (e.g. 10_5) is obtained

Analytical solution:

Nonlinear free vibration of laminated composite rectangular plates with curvilinear fibres

$$\frac{\omega}{\pi}\int_0^{2\pi/\omega} F(\omega,t)\cos(\omega t)dt = \left[\omega^2 M + K - \overset{\cup}{K}^T \overline{K}^{-1} \overset{\cup}{K} + \frac{3}{4}\overset{\approx}{K} - \frac{3}{4}\overset{\Lambda}{K}^T \overline{K}^{-1} \overset{\Lambda}{K}\right] Q$$

The properties of composite material is

$$E_1 = 1.03Tpa; E_2 = 4.05Gpa; \nu_{12} = 0.063; \nu_{21} = 0.4$$

$$Q_{11} = \frac{E_1}{1-\nu_{12}\nu_{21}} = 10.0566Gpa \qquad Q_{22} = \frac{E_2}{1-\nu_{12}\nu_{21}} = 4.154Gpa$$

$$Q_{12} = \nu_{12}Q_{22} = \nu_{21}Q_{11} = 0.2617Gpa$$

$$Q_{66} = G_{12} = 8.8Gpa$$

$$\bar{Q}_{11} = Q_{11}\cos^4(\theta) + 2(Q_{12} + 2Q_{66})\sin^2(\theta)\cos^2(\theta) + Q_{22}\sin^4(\theta)$$

$$\bar{Q}_{12} = (Q_{11} + Q_{22} - 4Q_{66})\sin^2(\theta)\cos^2(\theta) + Q_{12}(\sin^4(\theta) + \cos^4(\theta))$$

$$\bar{Q}_{22} = Q_{11}\sin^4(\theta) + 2(Q_{12} + 2Q_{66})\sin^2(\theta)\cos^2(\theta) + Q_{22}\cos^4(\theta)$$

$$\bar{Q}_{16} = (Q_{11} - Q_{12} - 2Q_{66})\sin(\theta)\cos^3(\theta) - (Q_{22} - Q_{12} - 2Q_{66})\sin^3(\theta)\cos(\theta)$$

$$\bar{Q}_{26} = (Q_{11} - Q_{12} - 2Q_{66})\sin^3(\theta)\cos(\theta) - (Q_{22} - Q_{12} - 2Q_{66})\sin(\theta)\cos^3(\theta)$$

$$\left[Q_{ij}\right]_{90} = \begin{bmatrix} 4.154 & 0.2617 & 0 \\ 0.2617 & 10.566 & 0 \\ 0 & 0 & 8.8 \end{bmatrix}$$

$$\left[Q_{ij}\right]_{45} = \begin{bmatrix} 12.610 & -4.8541 & 5.250 \\ -4.8541 & 12.610 & 5.250 \\ 5.250 & 5.250 & 3.5490 \end{bmatrix}$$

$$\left[Q_{ij}\right]_{0} = \begin{bmatrix} 10.566 & 0.2617 & 0 \\ 0.2617 & 4.154 & 0 \\ 0 & 0 & 8.8 \end{bmatrix}$$

$$\left[Q_{ij}\right]_{45} = \begin{bmatrix} 12.610 & -4.8541 & 1.6029 \\ -4.8541 & 12.610 & 1.6029 \\ 1.6029 & 1.6029 & 3.5490 \end{bmatrix}$$

Before going to next step I find ABD matrix

$$A_{IJ}=\sum_{K=1}^{N}(Z_{k+1}-Z_k)\bar{Q}_{ij}^{(k)}$$

$$B_{IJ}=\frac{1}{2}\sum_{K=1}^{N}(Z^2{}_{k+1}-Z^2{}_k)\bar{Q}_{ij}^{(k)}$$

$$D_{IJ}=\frac{1}{3}\sum_{K=1}^{N}(Z^3{}_{k+1}-Z^3{}_k)\bar{Q}_{ij}^{(k)}$$

$$A_{IJ}=\sum_{K=1}^{N}(Z_{k+1}-Z_k)\bar{Q}_{ij}^{(k)}=0.005*10^{-9}\begin{bmatrix}10.566 & 0.2617 & 0\\ 0.2617 & 4.154 & 0\\ 0 & 0 & 8.8\end{bmatrix}$$

$$B_{IJ}=\frac{1}{2}\sum_{K=1}^{N}(Z^2{}_{k+1}-Z^2{}_k)\bar{Q}_{ij}^{(k)}=0*\begin{bmatrix}10.566 & 0.2617 & 0\\ 0.2617 & 4.154 & 0\\ 0 & 0 & 8.8\end{bmatrix}$$

$$D_{IJ}=\frac{1}{3}\sum_{K=1}^{N}(Z^3{}_{k+1}-Z^3{}_k)\bar{Q}_{ij}^{(k)}=10.416*10^{-9}\begin{bmatrix}10.566 & 0.2617 & 0\\ 0.2617 & 4.154 & 0\\ 0 & 0 & 8.8\end{bmatrix}$$

Let considered 8 ply composite material P=8; i=j.

$$g_{j+1}(-1)=g_{j+1}(1)=0$$

$$\int_{-1}^{1}\frac{dg_{i+1}(\xi)}{d\xi}\frac{dg_{j+1}(\xi)}{d\xi}d\xi=\begin{cases}1 if i=j\\ 0 if i\neq j\end{cases}$$

$$g_1(\xi)=\frac{1}{2}(1-\xi)$$

$$g_2(\xi)=\frac{1}{2}(1+\xi)$$

$$g_{j+1}(\xi)=\sqrt{\frac{2j-1}{2}}\int_{-1}^{\xi}p_{j-1}(\zeta)d\zeta\,(j=2,3.....,p)$$

$$f_{j+1}(-1)=f_{j+1}(1)=\frac{df_{j+1}(-1)}{d\xi}=\frac{dg_{j+1}(1)}{d\xi}$$

$$\int_{-1}^{1}\frac{d^2f_{i+1}(\xi)}{d\xi^2}\frac{d^2f_{j+1}(\xi)}{d\xi^2}d\xi=\begin{cases}1 if i=j\\ 0 if i\neq j\end{cases}$$

$$f_1(\xi)=\frac{1}{4}(2-3\xi+\xi^3)$$

$$f_2(\xi)=\frac{1}{4}(1-\xi-\xi^2+\xi^3)$$

$$f_3(\xi)=\frac{1}{4}(2+3\xi-\xi^3)$$

$$f_4(\xi)=\frac{1}{4}(-1-\xi+\xi^2+\xi^3)$$

$$f_{j+1}(\xi)=\int_{-1}^{\xi}g_j(\zeta)d\zeta\,(j=4,5.....,p)$$

After we find stiffness matrix

$$\overline{K_{ij}} = \begin{bmatrix} \overline{K}_{2I-1,2J-1} & \overline{K}_{2I-1,2J} \\ \overline{K}_{2I,2J-1} & \overline{K}_{2I,2J} \end{bmatrix}$$

$$\overset{\cup}{K}_{ij} = \begin{bmatrix} \overset{\cup}{K}_{2i-1j} \\ \overset{\cup}{K}_{2IJ} \end{bmatrix}$$

$$\hat{K}_{ij} = \begin{bmatrix} \hat{K}_{2i-1j} \\ \hat{K}_{2IJ} \end{bmatrix}$$

$$f_1(\xi) = \frac{1}{4}(2 - 3\xi + \xi^3)$$

$$f_2(\xi) = \frac{1}{4}(1 - \xi - \xi^2 + \xi^3)$$

$$f_3(\xi) = \frac{1}{4}(2 + 3\xi - \xi^3)$$

$$f_4(\xi) = \frac{1}{4}(-1 - \xi + \xi^2 + \xi^3)$$

This values calculating from appendix A(from Elsevier journal Nonlinear free vibration of laminated composite rectangular plates with curvilinear fibers, A. Houmat)

To calculate stiffness matrix

a = 5nm ; b = 5nm ; h = 40nm ; =1.1 g/cm^(-3)

$$\overline{K}_{2I-1,2J} = 9.405*10^{-9}$$

$$\overline{K}_{2I-1,2J-1} = 2.6517*10^{-8}$$

$$\overline{K}_{2I,2J-1} = 9.40573*10^{-9} \quad \overline{K}_{2I,2J} = 1.79225*10^{-8}$$

$$\overline{K_{ij}} = \begin{bmatrix} 2.651*10^{-8} & 9.405*10^{9} \\ 9.405*10^{9} & 1.7922*10^{-8} \end{bmatrix}$$

$$\overset{\cup}{K}_{2i-1j} = 0 \qquad \overset{\cup}{K}_{2IJ} = 0$$

$$\overset{\cup}{K}_{ij} = \begin{bmatrix} 0 \\ 0 \end{bmatrix}$$

$$\hat{K}_{2i-1j} = 464.8499 \quad \hat{K}_{2IJ} = 3692.933$$

$$\hat{K}_{ij} = \begin{bmatrix} 464.8499 \\ 3692.933 \end{bmatrix}$$

$$\tilde{\tilde{K}} = 1569$$

$K_{IJ} = 1.2676*10\text{^}(10)$

M=1.2900*10^(-11)

All values are substitute below equation we get frequency of the material

$$\frac{\omega}{\pi}\int_0^{2\pi/\omega} F(\omega,t)\cos(\omega t)dt = \left[\omega^2 M + K - \overset{\cup}{K}^T \overline{K}^{-1} \overset{\cup}{K} + \frac{3}{4}\overset{\approx}{K} - \frac{3}{4}\overset{\Lambda}{K}^T \overline{K}^{-1} \overset{\Lambda}{K}\right] Q = 0$$

$$-\omega^2\left(1.2900*10^{-11}\right) + \left(1.2676*10^{10}\right) - 0 + \left[\frac{2}{3}(1569)\right] - \left[\frac{3}{2}(784.49)\right] = 0$$

$$\omega^2 = 9.8217X10^{20}$$

$$\omega = 3.13396X10^{10}\,Hz$$

Conclusion:

In this work we find the frequency of advanced composites. Using vonkarman's thin plate theory . this material revolving or exceeding mechanical and electrical properties of composite material. It having high thermal resistance ,high strength low density and extremely low coefficient of thermal expansion with compare to the carbon fibber composites . And also it restrict more vibrations . So this is use full aerospace application.

REFERENCES

Vibration characteristics of single-walled carbon nanotubes based on an anisotropic elastic shell model including chirality effect E. Ghavanloo, S.A. Fazelzadeh

Mechanical and electrical properties of aligned carbon nanotube/carbon matrix composites Zhou Zhou a, Xin Wang a,1, ShaghayeghFaraji b, Philip D. Bradford b, Qingwen Li c, Yuntian Zhu a.

Carbon nanotube–polymer composites: Chemistry, processing, mechanical and electrical properties Zdenko Spitalskya,1, DimitriosTasisb,KonstantinosPapagelisb, Costas Galiotisa,b

Nonlinear free vibration of laminated composite rectangular plates with curvilinear fibers, A. Houmat⇑